Amino→Imino Tautomerization upon in Vacuo Sublimation of 2-Methyltetrazole-Saccharinate as Probed by Matrix Isolation Infrared Spectroscopy

A. Ismael,[†,‡] A. Gómez-Zavaglia,[‡,§] A. Borba,[‡] M. L. S. Cristiano,[†] and R. Fausto*[,‡]

[†]CCMAR and Department of Chemistry and Pharmacy, F.C.T., University of Algarve, P-8005-039 Faro, Portugal

[‡]Department of Chemistry, University of Coimbra, P-3004-535 Coimbra, Portugal

[§]Center for Research, Development in Food Cryotechnology, Conicet La Plata, Universidad Nacional de La Plata, Ra-1900 La Plata, Argentina

S *Supporting Information*

ABSTRACT: The amino−imino tautomerization of the nitrogen-linked conjugate 2-methyltetrazole-saccharinate (2MTS) was observed upon sublimation of the compound in vacuo. As shown previously by X-ray diffraction [Ismael, A.; Paixão, J. A.; Fausto, R.; Cristiano, M. L. S. *J. Mol. Struct.*, **2011**, *1023*, 128−142], in the crystalline phase the compound exists in an amino-bridged tautomeric form. Infrared spectroscopic investigation of a cryogenic matrix prepared after sublimation of a crystalline sample of 2MTS and deposition of the sublimate together with argon (in ∼1:1000 molar ratio) onto an IR-transparent cold (15 K) substrate, revealed that the form of 2MTS present in the matrix corresponds to the theoretically predicted most stable imino-bridged tautomer. In this tautomer, the labile hydrogen atom is connected to the saccharine nitrogen, and the two heterocyclic fragments are linked by an imino moiety in which the double-bond is established with the carbon atom belonging to the saccharyl fragment. The observed isomeric form of this tautomer is characterized by a *zusammen* (Z) arrangement of the two rings around the C═N bond of the bridging group and an intramolecular NH···N hydrogen bond. The experimental IR spectrum of the matrix-isolated 2MTS has been fully assigned based on the calculated spectra for the two most stable conformers of this tautomer. A mechanism for the conversion of the tautomeric form existing in the crystal into that present in the gas phase is proposed. As a basis for the interpretation of the experimental results, a detailed theoretical [at the DFT(B3LYP) level of approximation with the 6-31++G(d,p) and 6-311++G(3df,3pd)] study of the potential energy surface of the compound was performed.
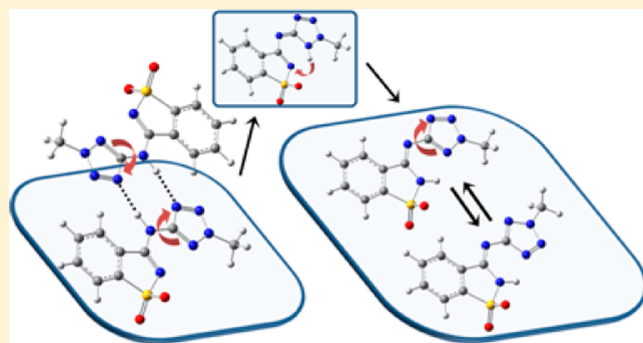
■ INTRODUCTION

Tetrazole-saccharinate conjugates have been emerging as useful ligands for coordination with transition metals,[1] which may have relevant applications in fields such as supramolecular chemistry[2] and molecular magnetism.[3] Recently, we devised synthetic routes to a small library of this type of compounds, where the two heterocyclic fragments are connected through a nitrogen bridge.[1,4,5] Very interestingly, it has been shown that the preferred tautomeric species of these compounds is very much determined by the chemical environment.[4,5] This property can be easily understood considering the variety of possible intra- and intermolecular interactions that may operate in these molecules, in particular of the H-bond type. Understanding the relevance of different tautomeric forms and possible conformations of these systems then appears of fundamental importance to explore their applications.

The parent nitrogen-bridged tetrazole-saccharinate conjugate was shown to exist preferentially as the (1*H*)-tetrazole iminosaccharin tautomer in the gas phase.[4] On the other hand, in the crystal it exists in the (1*H*)-tetrazole amino-saccharin tautomeric form.[4] In the isolated molecule, the main stabilizing interaction is the intramolecular H-bond between the NH group of the saccharyl moiety and the tetrazole ring. By contrast, the selected tautomer in the crystal is stabilized by an intricate network of hydrogen bonds, where the amino spacer is hydrogen bonded to the tetrazole group of a neighbor molecule and the NH group of the tetrazole fragment forms a bifurcated H-bond with the saccharyl nitrogen of the same molecule and with one of the oxygen atoms of a second neighbor.[4]

In the case of the derivative bearing a methyl group in position 2 of the tetrazole ring, nitrogen-bridged 2-methyltetrazole-saccharinate (abbreviated 2MTS), the amino-bridged tautomer was also found to be the species present in the

crystalline phase.[5] Dimers of 2MTS are linked through intermolecular hydrogen bonds involving the NH spacer group of each monomeric unit as proton donor and the tetrazole ring of the second molecule as acceptor (Figure 1).

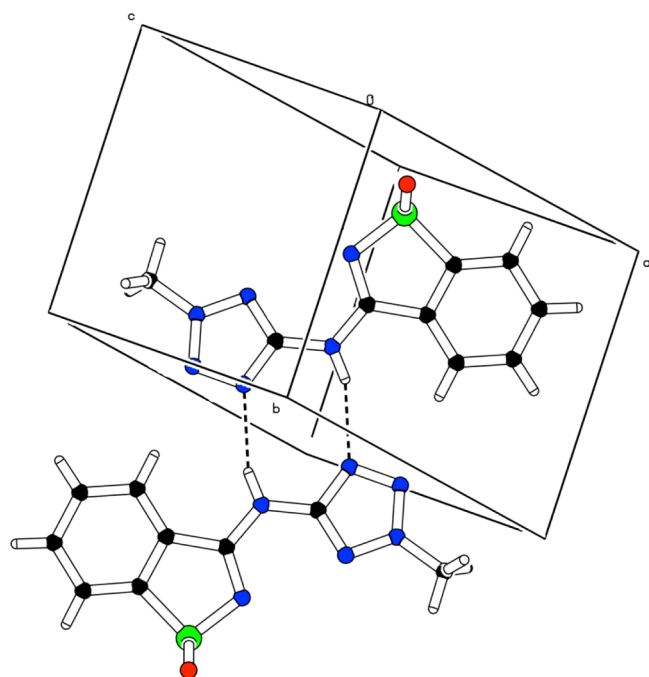**Figure 1.** Hydrogen bond network in 2MTS crystal.[5]

The unit present in the crystal is then similar to that found for the parent compound.[4] Also in a similar way to what has been previously found for the unsubstituted molecule,[4] DFT-(B3LYP)/6-31++G(d,p) calculations performed on 2MTS predicted the imino-bridged tautomer as the most stable species for the isolated molecule.[5] It could then be expected that 2MTS should also exist in this tautomeric form in the gas phase.

Since the presence of the methyl substituent in the tetrazole ring of 2MTS reduces the number of possible tautomers relatively to the unsubstituted compound, the methyl derivative appeared as an adequate target to explore in a deeper detail the tautomerism in this type of conjugates. Hence, in this study we have undertaken a detailed theoretical structural characterization of 2MTS and, subsequently, identified its structure in the gas phase by analysis of the infrared spectrum of the matrix-isolated compound. As shown in detail below, it could be doubtlessly demonstrated that, in the gas phase, 2MTS exists as the theoretically predicted most stable imino-bridged form. A mechanism for the conversion of the tautomeric form existing in the crystal into that present in the gas phase is proposed.

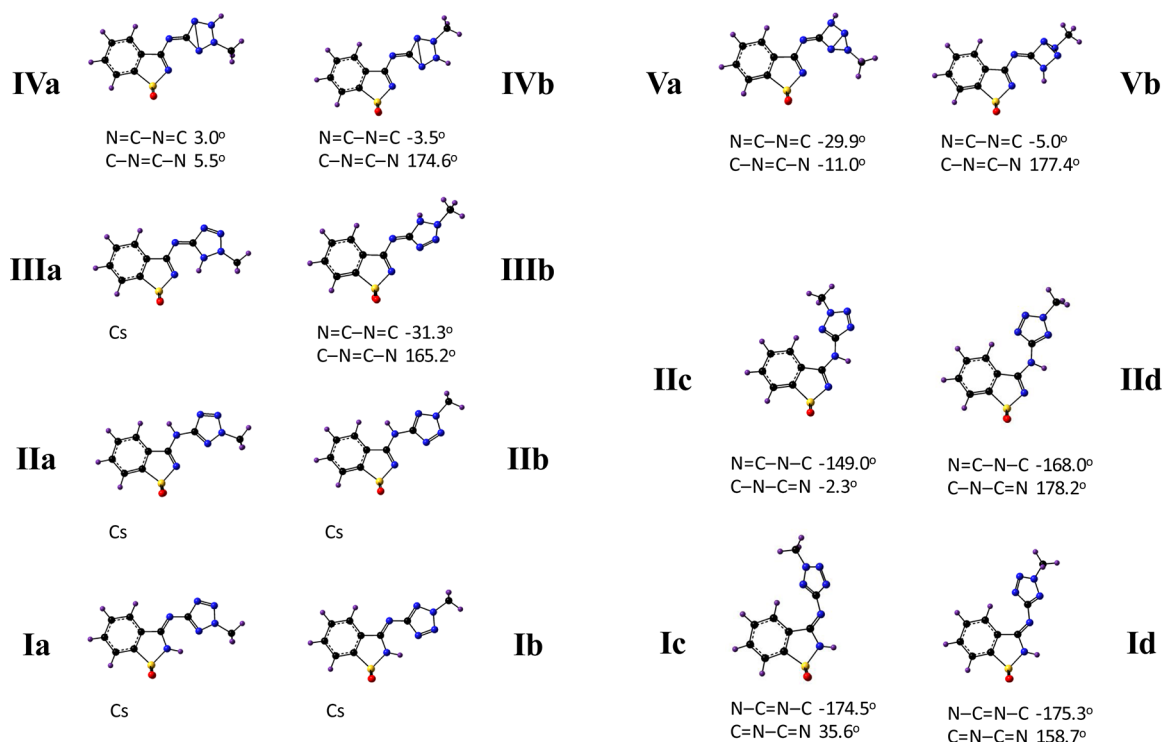## ■ EXPERIMENTAL AND COMPUTATIONAL METHODS

Figure 2. Possible tautomers of 2MTS (**I−V**) with the corresponding isomeric (structural or conformational) forms (**a−d**). The *entgengen* (**c,d**) forms of **III**, **IV**, and **V** correspond to high-energy forms (see text) and are not represented. The indicated dihedral angles about the bridge bonds were obtained at the B3LYP/6-31G++(d,p) level of theory. The angles are not given for forms with a planar molecular skeleton (Cs point group). For relative energies of the different forms, see Table 1. Optimized geometries are provided in Table S1 (Supporting Information).

The low-temperature matrices were prepared by codeposition, onto the cooled CsI substrate of the cryostat, of the matrix gas (argon 99.9998%, obtained from Air Liquide) and vapors of 2MTS produced by sublimation in a specially designed temperature variable mini-oven assembled inside the cryostat. The temperature of the mini-oven used for evaporation of the compounds was ca. 150 °C. The cryogenic system was based on an APD Cryogenics close-cycle helium refrigeration system with a DE-202A expander. The temperature of the CsI substrate during deposition was 15 K. The infrared spectra were obtained using a Nicolet 6700 Fourier transform infrared spectrometer equipped with a deuterated triglycinesulphate (DTGS) detector and a Ge/KBr beamsplitter, with 0.5 cm^{-1} spectral resolution.

The quantum chemical calculations were performed at the DFT level of theory using either the valence double-ζ polarized 6-31++G(d,p) or the extended valence triple-ζ polarized 6-311++G(3df,3pd) basis set[6−10] and the B3LYP functional.[11,12] Inclusion of both diffuse and polarization functions in the basis sets is required for a more accurate approximation to the calculated infrared spectra, since vibrational modes involving hypervalent S atoms (in particular the >SO$_2$ stretching modes) are known not to be correctly predicted at a lower level of approximation.[13−16] Geometries were optimized using the Direct Inversion in the Iterative Subspace (DIIS) method,[17] the potential energy profiles for the different investigated processes being obtained by means of the intrinsic reaction coordinate (IRC) method.[18,19] The transition states were located using the synchronous transit quasi-Newton method (QST3 implementation).[20,21] The optimization of geometries was followed by harmonic vibrational calculations undertaken at the same theory level. The nature of the obtained stationary points was checked through analysis of the corresponding Hessian matrix. The calculated harmonic vibrational frequencies (scaled by the factor 0.978, except for νN−H, for which the used scale factor was 0.938) were used to assist the analysis of the experimental spectra and to account for the zero-point vibrational energy (ZPVE) corrections. All calculations were performed with the Gaussian 03 suite of programs.[22]

■ RESULTS AND DISCUSSION

Tautomerism and Isomerism (Structural and Conformational) in 2MTS: Structural Characterization of the Compound. 2MTS has five possible tautomeric forms (Figure 2; see also Table S1 in the Supporting Information for optimized geometries of the different forms), each one exhibiting four different isomeric structures (either structural or conformational). According to the calculations, in the most stable tautomer of the compound (**I** in Figure 2), the labile hydrogen atom is attached to the saccharine nitrogen. In this form, the two heterocyclic fragments are linked by an imino moiety in which the double-bond is established with the carbon atom of the saccharyl fragment. In the lowest energy isomeric form of this tautomer, the two rings assume a *zusammen* (Z) arrangement around the C=N bond of the bridging group. Depending on the orientation of the tetrazole ring, two different conformers of this species may exist (**Ia** and **Ib**; see Figure 2), which correspond to the two lowest energy structures of 2MTS. Both **Ia** and **Ib** exhibit an intramolecular NH···N hydrogen bond, which largely contributes to their stabilization. Two conformers analogous to these low-energy forms, but where the arrangement about the C=N imino linkage is *entgengen* (E), also exist (**Ic; Id**). However, their

energies are much higher (ca. 40 kJ mol^{-1}; see Table 1), mainly because of the steric hindrance resulting from the close proximity of the tetrazole ring and the phenyl group of the saccharyl moiety.

Table 1. Relative Energies (ΔE), Zero-Point Corrected Relative Energies (ΔE°), and Relative Gibbs Energies at T = 150 °C (ΔG$_{(150)}$°) for the Various Tautomers of 2MTS^{a}

	ΔE	ΔE°	ΔG$_{(150)}$°
Ia	7.7 (7.4)	7.1 (6.9)	2.3 (6.1)
Ib	0.0 (0.0)	0.0 (0.0)	0.0 (0.0)
IIa	18.9 (15.7)	20.3 (17.1)	19.8 (14.6)
IIb	30.7 (26.7)	31.6 (27.7)	29.2 (18.2)
IIIa	81.8	78.0	79.0
IIIb	141.3	138.7	138.4
IVa	197.1	194.6	191.8
IVb	198.8	196.2	192.3
Va	405.2	397.4	399.2
Vb	388.4	381.1	384.8
Ic	46.9	46.3	45.6
Id	39.0	38.8	38.8
IIc	29.9	31.7	30.7
IId	27.8	30.2	27.2

^{a}All values are in kJ mol^{-1}. B3LYP/6-31++G(d,p) calculations. Values in parentheses were obtained at the B3LYP/6-311++G(3df,3pd) level of theory. The B3LYP/6-31++G(d,p) calculated absolute values of E, $E°$ and $G_{(150)}$° for the most stable form, **Ib**, are −1224.854632, −1224.671350, and −1224.742365 hartree, respectively; at the B3LYP/6-311++G(3df,3pd), these values are −1225.171291, −1224.987660, and −1225.057712 hartree. 1 hartree = 2625.5001 kJ mol^{-1}.

Other imino-bridged tautomers of the compound do also exist, where the labile hydrogen atom occupies the different available positions at the tetrazole ring (**III, IV, V**; see Figure 2). In all these forms, the C=N bond of the imino bridge is established with the tetrazole carbon atom. When the hydrogen is in positions 3 or 4, the resulting tautomeric forms (**IV, V**) have highly strained Dewar-tetrazole bicyclic structures, thus corresponding to high-energy species with relative energies larger than ca. 200 kJ mol^{-1} or 400 kJ mol^{-1}, respectively. However, when the hydrogen atom occupies the position 1 of the tetrazole ring (**III**; Figure 2), the situation is different, and the resulting isomer exhibiting an intramolecular NH···N hydrogen bond (where the saccharyl nitrogen atom acts as acceptor; **IIIa** in Figure 2) has a comparatively lower relative energy (∼80 kJ mol^{-1}). Note that, on the other hand, form **IIIb** has no intramolecular H-bond and has a much higher relative energy (∼140 kJ mol^{-1}), with the two heterocyclic rings considerably deviated from the planarity. For tautomers **III, IV**, and **V**, isomeric structures with the *entgengen* arrangement about the N=C bridge bond (of types **c** and **d**, according to the notation used in Figure 2) do also exist, but their relative energies are expectably very high (over ca. 200 kJ mol^{-1}).

The labile hydrogen atom can also be attached to the bridging nitrogen atom (**II**, Figure 2). In this case, the spacer between the saccharyl and tetrazole rings is an amino group. Internal rotations around the two C−N bridging bonds lead to the existence of four different conformers with predicted energies ranging from ca. 20 to 30 kJ mol^{-1}. Very interestingly, in the room temperature crystalline phase of the compound, 2MTS molecules were found to exist in the amino-bridged

form **IIa**, which allows for a more efficient packing.[5] In the crystal, the structure consists of a packing of dimeric centrosymmetric units, the dimers being formed via hydrogen bonding involving the NH group of the spacer of one of the units of the dimer and the nitrogen 4 of the tetrazole ring of the second unit (and vice versa). The estimated H-bond energy per H-bond in the crystal was found to be 13.3 kJ mol^{-1}.[5]

According to the calculations, for the isolated molecule, the most stable form is **Ib**. The second most stable species is form **Ia**, which differs from the most stable form by a 180° internal rotation around the bridging N−C bond. Both forms have a planar heavy atom skeleton and bear an intramolecular N−H⋯N hydrogen bond. The potential energy profile for the interconversion between these two forms is depicted in Figure 3. As shown in this figure, the B3LYP/6-31++G(d,p) barrier for the **Ib**→**Ia** conformational isomerization amounts to 35.7 kJ mol^{-1} (28.0 kJ mol^{-1} in the reverse direction).
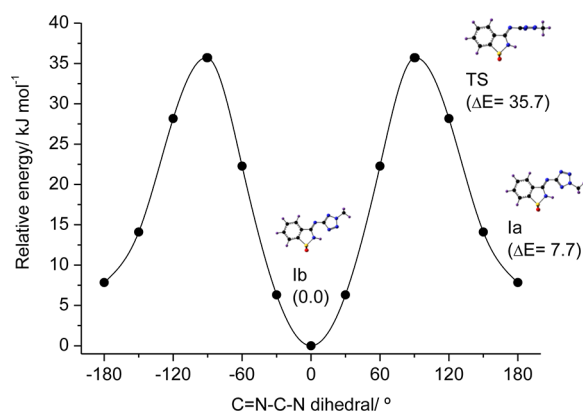
Figure 3. B3LYP/6-31++G(d,p) calculated potential energy profile for the **Ia**−**Ib** conformational isomerization in 2MTS.

Table 2 shows some relevant molecular parameters for characterization of the intramolecular H-bonds in forms **Ia** and **Ib**, as well as for forms **IIIa** and **Vb** that also have geometric arrangements compatible with the existence of such type of interaction (see Figure 2). As it could be expected, all parameters indicate that the H-bond is stronger in the most stable form (**Ib**) than in **Ia**: in form **Ib** the N−H and H⋯N distances are shorter and longer than in **Ia**, respectively, while the ∠N−H⋯N angle is larger and the charge on the H atom is more positive. In addition, the charge on the donor N atom is more negative in form **Ib**, evidencing the greater localization of the charge on this atom at expenses of the N−H bond. Furthermore, the charge on the acceptor N atom is less negative, indicating the migration of electron charge from this atom toward the H⋯N hydrogen bond. Very interestingly, the

data shown in Table 2 also indicate that among all the forms of 2MTS bearing an intramolecular H-bond, form **IIIa** is the one where this interaction is the strongest. In this case, the charges on the N atoms are not directly comparable with those of **Ia** and **Ib** because the donor and acceptor atoms are different. However, both the values of the charge on the H atom and the bond distances are quite illustrative of the greater strength of the H-bond in **IIIa** compared to **Ia** and **Ib**. The results also show that if it exists, the H-bond in form **Vb** is very weak.

Preferred Structure of 2MTS in the Gas Phase: Matrix Isolation Infrared Spectroscopy Experiments. As mentioned in the previous section, in the room temperature crystalline phase, 2MTS exists in the amino-bridged form **IIa**. Since the theoretical calculations performed on the compound predicted that the lowest energy tautomer of the compound in gas phase should correspond to imino-bridged tautomer **I**, a sample of crystalline 2MTS was sublimated in vacuo, and the obtained vapors of the compound were deposited together with argon (in a ca. 1:1000 molar ratio) onto a substrate kept at 15 K (see details in the Experimental and Computational Methods section), and investigated spectroscopically to structurally characterize the sublimate. The infrared spectrum of the argon matrix of 2MTS prepared this way is presented in Figure 4a.

The comparison of the spectrum of the matrix with those theoretically obtained for the different forms of 2MTS revealed that the experimental spectrum corresponds to a mixture of the two lowest energy conformers of the imino-bridged tautomer **I** (**Ia**, **Ib**). The B3LYP/6-311++G(3df,3pd) calculated infrared spectra of forms **Ia** and **Ib** are drawn as stick spectra in Figure 4c. A simulated spectrum, built by adding the calculated spectra of these two forms with intensities weighted assuming a **Ib**/**Ia** population ratio of 0.72/0.28, is presented in Figure 4b. The population ratio was obtained from the observed relative intensities of the νN−H bands ascribed to each conformer (which appear well separated in the experimental spectrum), normalized by the corresponding theoretical infrared intensities calculated at the B3LYP/6-311++G(3df,3pd). This population ratio agrees fairly well with that predicted for the gas phase equilibrium between the two conformers (**Ia**, **Ib**) at the temperature of sublimation of the compound using the B3LYP/6-31G++(d,p) calculated $\Delta G_{(150)}^{\circ}$ values: 0.66/0.34 (the larger 6-311++G(3df,3pd) basis set predicted a somewhat larger relative population of **Ib**, with **Ib**/**Ia**= 0.86/0.14).

It is clear from Figure 4 that the simulated spectrum fits the observed one very well. Though the spectral signatures of forms **Ia** and **Ib** are very similar, there are a few spectral regions that can be used to doubtlessly establish the presence of the two conformers in the matrix (see Tables S2−S5 in the Supporting Information for complete calculated vibrational data for forms

Table 2. B3LYP/6-31++G(d,p) Calculated Intramolecular Hydrogen Bond Parameters for the 2MTS forms Ia, Ib, IIIa and Vb[a]

	Ia	Ib	IIIa	Vb
N−H	1.018 (1.014)	1.022 (1.017)	1.037	1.016
H⋯N	2.075 (2.067)	2.027 (2.022)	1.832	2.466
∠N−H⋯N	120.3 (121.1)	122.0 (122.7)	120.7	95.4
$q_{(N)}$ donor	−0.717 (−0.955)	−0.759 (−0.992)	−0.683	−0.282
$q_{(H)}$⋯	+0.432 (+0.592)	+0.435 (+0.603)	+0.483	+0.375
$q_{(N)}$ acceptor	−0.720 (−0.862)	−0.614 (−0.579)	−0.558	−0.574

[a]Distances in Å; angles in degrees; Mulliken charges on the atoms in units of electron (1e = 1.60217646 × 10^{-19} C). For **Ia** and **Ib**, the values in parentheses were obtained at the B3LYP/6-311++G(3df,3pd) level of theory.

D

dx.doi.org/10.1021/jp401360c | J. Phys. Chem. A XXXX, XXX, XXX−XXX
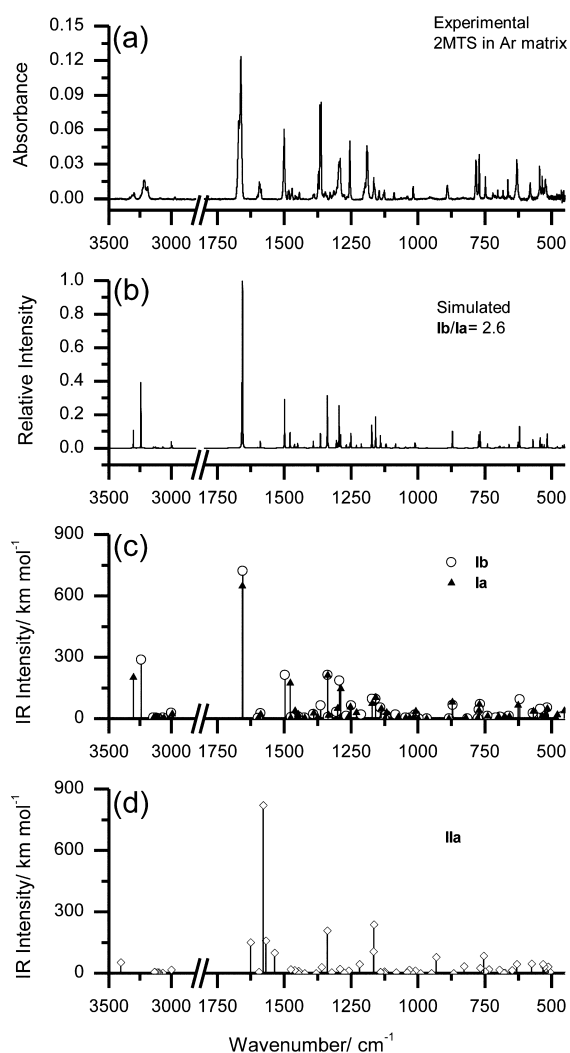
Figure 4. (a) Infrared spectrum of the as-deposited argon matrix (15 K) of 2MTS. (b) Normalized to unit simulated infrared spectrum built from the B3LYP/6-311++G(3df,3pd) calculated IR spectra of forms **Ia** and **Ib** (shown in panel c as stick spectra), with intensities scaled by the ratio **Ib/Ia**=2.6 (see text). (d) B3LYP/6-311++G(3df,3pd) calculated IR spectrum of form **IIa**. In the simulated spectrum, bands were simulated by Lorentzian functions with full bandwidth at half-maximum equal to 1 cm^{-1}, centered at the calculated wavenumbers (scaled by 0.978 except in the νN−H stretching region where the scale factor used was 0.938).

Ia and **Ib** and detailed assignment of the observed spectrum). In the νNH stretching region, the two conformers give rise to well-separated features (structured bands resulting from matrix-site splitting). In agreement with the stronger N−H···N intramolecular hydrogen bond in conformer **Ib**, the νNH stretching mode of this form appears at a considerably lower frequency ($\sim$3210 cm^{-1}) than in form **Ia** ($\sim$3300 cm^{-1}). In turn, the bridge νC=N stretching mode in both conformers is shown by the vibrational calculations to be coupled in some extent with the in-plane bending of the H-bonded N−H group (see Tables S3 and S4). Because of that, this vibration appears at experimentally discernible frequencies in the two conformers. In agreement with the calculations, form **Ia** absorbs at a slightly higher frequency (1670 cm^{-1}), while the higher intensity band at (1662 cm^{-1}) is ascribed to the most abundant form **Ib**. Other bands assigned exclusively to the less abundant form **Ia** are observed in the 1480−1470 cm^{-1} region (mostly bridge νN−C

stretching), and at 1362 (νSO$_2$ antisymmetric stretching), 1303 (with an important contribution of the saccharyl νC−N stretching), 1291 (H-bonded δN−H in-plane bending), 1188 (νSO$_2$ symmetric stretching), 1017/1016 (predominantly tetrazole νN−N and νC−N stretchings mixed with a γCH$_3$ rocking mode), 711 (principally νS−C stretching), 678 (νN−C(H$_3$) stretching), 636 (νN−S stretching), 480 (H-bonded γN−H out-of-plane bending), and 456 (delocalized mode, also with a significant contribution from the γN−H out-of-plane bending coordinate) cm^{-1}. All these bands are observed at positions fitting well their predicted positions (1478, 1337, 1300, 1288, 1171, 1008, 698, 678, 626, 477, and 451 cm^{-1}, respectively).

Note that the calculated spectrum for the 2MTS crystalline phase relevant form **IIa** (and also those predicted for the other amino-bridged higher-energy conformers, **IIb**, **IIc**, and **IId**) is markedly different from the experimentally observed spectrum (see Figure 4d). This is particularly noticeable in the νN−H stretching region and the 1630−1500 cm^{-1} range. In the first case, **IIa** is predicted by the calculations to give rise to a band at ca. 3400 cm^{-1} (typical for a non-hydrogen bonded N−H group) where no corresponding absorptions were found in the experimental spectrum. In the second case, according to the calculations **IIa** should give rise to four intense bands in the 1630−1500 cm^{-1} region (at 1626, 1579, 1569, and 1537 cm^{-1}), while in the experimental spectrum only one band was observed (which is ascribable to a phenyl νCC stretching mode of tautomer **I** forms).

In conclusion, the experimental results doubtlessly demonstrate that, upon in vacuo sublimation of 2MTS in an effusive-type cell, tautometization takes place, transforming the crystal phase **IIa** into tautomer **I**. Under the experimental conditions used, the two lowest energy conformers of **I** (**Ia** and **Ib**) approach their relative populations of thermodynamic equilibrium in the gas phase at the temperature of sublimation, suggesting a high collision rate in the gaseous beam seeding region. The observed tautomerization follows the previously reported (amino-bridged)→(imino-bridged) tautomerization upon sublimation of the parent tetrazole-saccharinate,[4] and seems then to be a relatively general phenomenon in this type of conjugates.

To establish a mechanism for the observed tautomerization is a difficult task, in particular because one can expect that it takes place (at least partially) in the condensed phase or at the solid−gas interface. In any case, for the specific system under study it was possible to obtain enough structural and energetic information that can be used to propose a possible route leading to the observed conversion of **IIa** into **Ia** and **Ib**.

The first point to notice is that no evidence of the presence in the gas phase of tautomer **II** (either of its conformer **IIa** or any other conformer of this tautomeric form, i.e., **IIb**, **IIc**, **IId**) was obtained. This fact suggests that tautomer **II** is not released from the crystal into the gas phase, at least as a monomer. The second point to note, is that the location of the labile hydrogen atom in the form existing in the crystal of 2MTS (**IIa**) is not appropriate for its direct migration to the saccharyl nitrogen atom, where it is attached in tautomer **I**. For a direct migration of the hydrogen, one has to assume that **IIa** should first convert into **IIc** by internal rotation around the bridge C$_{(saccharyl)}$−N bond. The calculated barrier for such rotamerization amounts to 49.3 kJ mol^{-1} (B3LYP/6-31++G(d,p) results), which is low enough to be overcome in the gas phase at the temperature used to sublimate the compound in the present experiments.
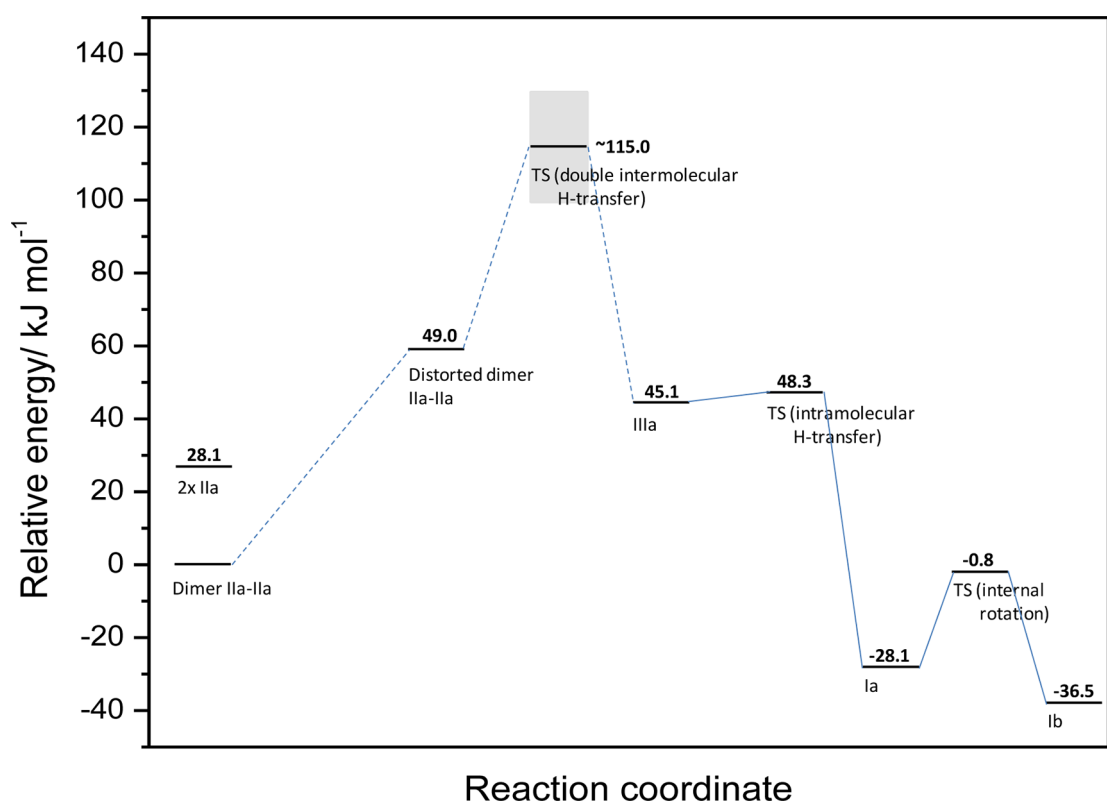
Figure 5. Proposed mechanism for conversion of tautomer **IIa**, existing in crystalline 2MTS,[5] into the experimentally observed forms **Ia** and **Ib**, existing in the gas phase. A barrier for double proton transfer in the range 50−80 kJ mol^{-1} is assumed in the scheme (see text).

However, starting from **IIc** (or from **IId**, assuming the conversion of **IIc** into **IId**, whose associated calculated barrier is only 7.0 kJ mol^{-1}), the resulting tautomer **I** formed after the required migration of the hydrogen atom from the bridging group to the saccharyl nitrogen atom would be **Ic** (or **Id**). The calculated H-transfer barrier (converting **IIc** into **Ic**) amounts to 186 kJ mol^{-1}. In addition, conversion of **Ic** (or **Id**), with an *E* configuration about the C═N bridge moiety, into the observed **Ia** (or **Ib**) forms, with the *Z* configuration, is a highly improbable thermal process, with a high energy barrier (over 250 kJ mol^{-1}).[23,24] Under these conditions, an alternative route resulting in the observed tautomeric conversion must exist.

In the mechanism here proposed, schematically depicted in Figure 5, the fact that the main constituting unit of the MTS2 crystal is a **IIa** dimer[5] is of fundamental importance. As shown in Figure 1, in this dimer the molecules are linked through intermolecular hydrogen bonds involving the amine N−H spacer group of each monomeric unit as proton donor and the nitrogen at position 4 of the tetrazole ring of the second molecule as acceptor. Besides, the saccharyl and tetrazole rings are not coplanar,[5] but distorted through internal rotation around the most flexible N−C$_{(tetrazole)}$ bond of the bridge by about 15° (the calculated torsional vibration associated with the internal rotation about this bond is as small as ca. 25 cm^{-1}, proving that large amplitude movements are allowed about this coordinate). We calculated the rise of energy in the dimer upon further increase of the angle of internal rotation about this flexible N−C$_{(tetrazole)}$ bond until a nearly perpendicular orientation of the two rings. The obtained value, 49 kJ mol^{-1}, is well within the range of energies surpassable during sublimation.[25] At this geometry, a double proton-transfer can take place within the dimeric unit, from the amino spacer-group

of each molecule to the tetrazole nitrogen atom in position 1 of the second molecule, instead of to that in position 4. The transfer to the nitrogen in position 4 would in fact be the result of the direct intradimer double proton-transfer for the dimeric structure existing in the crystal (see Figure 1). However, the species resulting from that process would be the high-energy tautomer **V** (see Table 1), and such process is certainly not energetically accessible. On the other hand, the tautomer produced upon proton transfer to the nitrogen in position 1 of the tetrazole is form **IIIa**, which has a much lower energy. Assuming that the double proton-transfer process has an energy barrier between 50 and 80 kJ mol^{-1}, as found for other nitrogen containing heterocyclic dimers,[26−29] one can roughly estimate the energetic demand for production of a **IIIa** unit of 2MTS in the gas phase from a **IIa** unit in the crystal as being within 100−130 kJ mol^{-1} (see Figure 5). This appears as a meaningful accessible energy value for the considered process.[25,29,30] Once produced, **IIIa** can then be promptly converted into **Ia** by intramolecular H-transfer in the gas phase. The calculated potential energy profile for this reaction is shown in Figure 6, and shows a **IIIa→Ia** barrier of only 3.2 kJ mol^{-1}. Finally, once **Ia** is obtained, an equilibrium between **Ia** and **Ib** can be established, as discussed above, leading to the sole observation of these two forms.

It is important to note that the low barrier associated with the considerably exothermic **IIIa→Ia** conversion implies that this step is a fast process obeying the Hammond−Leffler postulate,[31,32] i.e., the associated transition state corresponds to an early transition state structurally resembling more the higher-energy reactant (**IIIa**) than the product (**Ia**).

It shall also be pointed out that the involvement of dimeric units in tautomerization processes associated with sublimation
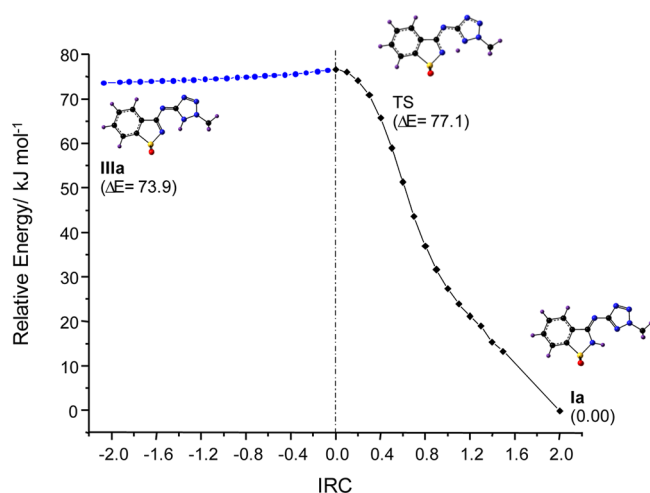
Figure 6. Potential energy profile for the intramolecular proton transfer converting 2MTS form **IIIa** into form **Ia**, obtained in the performed B3LYP/6-31++G(d,p) IRC calculations.

has received both experimental and computational support in the last years, including for tetrazole-based compounds.[29,33,34] Furthermore, it has also been suggested that double H-transfer type processes in hydrogen bonded complexes, like the one herein proposed to take place during sublimation of 2MTS, shall play an especially important role in the aggregated phase.[29] This is also in agreement with the absence of tautomer **II** of 2MTS in the gas phase, as doubtlessly shown in the present matrix-isolation experiments.

CONCLUSIONS

2MTS was found to undergo complete amino−imino tautomerization upon sublimation, where the amino-bridged tautomeric form **IIa** existing in the crystalline phase of the compound is converted into a mixture of two conformers of the theoretically predicted most stable imino-bridged tautomer (**Ia**, **Ib**). In this tautomer, the labile hydrogen atom is connected to the saccharine nitrogen, and the two heterocyclic fragments are linked by an imino moiety in which the double-bond is established with the carbon atom belonging to the saccharyl fragment. The observed isomeric forms of this tautomer are characterized by a *zusammen* (*Z*) arrangement of the two rings around the C=N bond of the bridging group and an intramolecular NH···N hydrogen bond.

A simplified mechanism for the observed tautomeric conversion was proposed, which implies a partial internal rotation about the flexible bridging N−C$_{(tetrazole)}$ bond of the two molecules in the dimer, followed by a concerted double H-transfer in the deformed dimeric structure, leading to the formation of two units of tautomer **IIIa**, in a process whose energetic demand for production of a **IIIa** unit of 2MTS in the gas phase from a **IIa** unit in the crystal could be roughly estimated to be within 100−130 kJ mol^{-1}. The produced tautomer **IIIa** can then promptly convert into tautomeric form **Ia** in the gas phase in a low-barrier (3.2 kJ mol^{-1}) intramolecular H-transfer. Once **Ia** is obtained from **IIIa**, an equilibrium between **Ia** and **Ib** can be established by internal rotation about the N−C$_{(tetrazole)}$ bond in a process with an estimated energy barrier of ~28 kJ mol^{-1} (in the **Ia**→**Ib** direction).

The proposed mechanism implies the involvement of the dimer of the compound in the tautomerization accompanying the sublimation, and is consistent with recent experimental and computational evidence for similar processes in other compounds, including other tetrazole-based substances.[29,31,32]

Finally, the experimental IR spectrum of the matrix-isolated 2MTS has been fully assigned based on the B3LYP/6-311++G(2df,3pd) calculated spectra for the relevant forms of the compound (**Ia**, **Ib**).

ASSOCIATED CONTENT

Ⓢ Supporting Information

Table S1, with optimized Cartesian coordinates of the different tautomeric forms of 2MTS; Tables S2−S4, with the results of the normal coordinate analyses performed on the two experimentally relevant forms of 2MTS, **Ia** and **Ib**, based on the B3LYP/6-311++G(3df,3pd) optimized geometries and harmonic force constants; Table S5, with the assignment of the observed infrared spectrum of 2MTS in an argon matrix. This material is available free of charge via the Internet at http://pubs.acs.org.

AUTHOR INFORMATION

Corresponding Author
*E-mail: rfausto@ci.uc.pt.

Notes
The authors declare no competing financial interest.

ACKNOWLEDGMENTS

REFERENCES

(1) Frija, L. M. T.; Fausto, R.; Loureiro, R. M. S.; Cristiano, M. L. S. Synthesis and Structure of Novel Benzisothiazole-Tetrazolyl Derivatives for Potential Application as Nitrogen Ligands. *J. Mol. Catal. A: Chem.* **2009**, *305*, 142−146.

(2) Lehn, J.-M., Ed. *Supramolecular Chemistry*; Verlag Wiley-VCH: Weinheim, Germany, 1995.

(3) Kahn, O., Ed. *Magnetism: A Supramolecular Function*; Kluwer Academic Publishers: Dordrecht, The Netherlands, 1996.

(4) Gómez-Zavaglia, A.; Ismael, A.; Cabral, L. I. L.; Kaczor, A.; Paixão, J. A.; Fausto, R.; Cristiano, M. L. S. Structural Investigation of Nitrogen-Linked Saccharinate-Tetrazole. *J. Mol. Struct.* **2011**, *1003*, 103−110.

(5) Ismael, A.; Paixão, J. A.; Fausto, R.; Cristiano, M. L. S. Molecular Structure of Nitrogen-Linked Methyltetrazole-Saccharinates. *J. Mol. Struct.* **2012**, *1023*, 128−142.

(6) Krishnan, R.; Binkley, J. S.; Seeger, R.; Pople, J. A. Self-Consistent Molecular Orbital Methods. XX. A Basis Set for Correlated Wave Functions. *J. Chem. Phys.* **1980**, *72*, 650−654.

(7) McLean, A. D.; Chandler, G. S. Contracted Gaussian Basis Sets for Molecular Calculations. I. Second Row Atoms, Z = 11−18. *J. Chem. Phys.* **1980**, *72*, 5639−5648.

(8) Frisch, M. J.; Pople, J. A.; Binkley, J. S. Self-Consistent Molecular Orbital Methods 25. Supplementary Functions for Gaussian Basis Sets. *J. Chem. Phys.* **1984**, *80*, 3265−3269.

(9) Clark, T.; Chandrasekhar, J.; Spitznagel, G. W.; Schleyer, P. v. R. Efficient Diffuse Function-Augmented Basis Sets for Anion Calculations. III. The 3-21+G Basis Set for First-Row Elements, Li−F. *J. Comput. Chem.* **1983**, *4*, 294−301.

(10) Gill, P. M. W.; Johnson, B. G.; Pople, J. A.; Frisch, M. J. The Performance of the Becke−Lee−Yang−Parr (B-LYP) Density Functional Theory with Various Basis Sets. *Chem. Phys. Lett.* **1992**, *197*, 499−505.

(11) Becke, A. D. Density-Functional Exchange-Energy Approximation with Correct Asymptotic Behavior. *Phys. Rev. A* **1988**, *38*, 3098−3100.

(12) Lee, C. T.; Yang, W. T.; Parr, R. G. Development of the Colle−Salvetti Correlation-Energy Formula into a Functional of the Electron Density. *Phys. Rev. B* **1988**, *37*, 785−789.

(13) Kaczor, A.; Almeida, R.; Gómez-Zavaglia, A.; Cristiano, M. L. S.; Fausto, R. Molecular Structure and Infrared Spectra of the Monomeric Pseudosaccharin 3-(Methoxy)-1,2-benzisothiazole 1,1-Dioxide (Methyl Pseudosaccharyl Ether). *J. Mol. Struct.* **2008**, *876*, 77−85.

(14) Gómez-Zavaglia, A.; Kaczor, A.; Almeida, R.; Cristiano, M. L. S.; Fausto, R. Conformational Space of the *Pseudo*saccharin Allyl Ether 3-(Allyloxy)-1,2-benzisothiazole 1,1-Dioxide In Gas Phase and in Rare Gas Matrices. *J. Phys. Chem. A* **2008**, *112*, 1762−1772.

(15) Gómez-Zavaglia, A.; Kaczor, A.; Coelho, D.; Cristiano, M. L. S.; Fausto, R. Conformational and Structural Analysis of 2-Allyl-1,2-benzisothiazol-3(2*H*)-one 1,1-Dioxide as Probed by Matrix-Isolation Spectroscopy and Quantum Chemical Calculations. *J. Mol. Struct.* **2009**, *919*, 271−276.

(16) Gómez-Zavaglia, A.; Kaczor, A.; Almeida, R.; Cristiano, M. L. S.; Eusébio, M. E. S.; Maria, T. M. R.; Mobili, P.; Fausto, R. The Thermally Induced Sigmatropic Isomerization of Pseudosaccharyl Allylic Ether. *J. Phys. Chem. A* **2009**, *113*, 3517−3522.

(17) Pulay, P. Improved SCF Convergence Acceleration. *J. Comput. Chem.* **1982**, *3*, 556−560.

(18) Fukui, K. The Path of Chemical Reactions - The IRC approach. *Acc. Chem. Res.* **1981**, *14*, 363−368.

(19) Hratchian, H. P.; Schlegel, H. B. Finding Minima, Transition States, and Following Reaction Pathways on *Ab Initio* Potential Energy Surfaces. In *Theory and Applications of Computational Chemistry: The First 40 Years*; Dykstra, C. E., Frenking, G., Kim, K. S., Scuseria, G., Eds.; Elsevier: Amsterdam, 2005; pp 195−249.

(20) Peng, C.; Schlegel, H. B. Combining Synchronous Transit and Quasi-Newton Methods for Finding Transition States. *Israel J. Chem.* **1993**, *33*, 449−454.

(21) Peng, C.; Ayala, P. Y.; Schlegel, H. B.; Frisch, M. J. Using Redundant Internal Coordinates to Optimize Equilibrium Geometries and Transition States. *J. Comput. Chem.* **1996**, *17*, 49−56.

(22) Frisch, M. J.; Trucks, G. W.; Schlegel, H. B.; Scuseria, G. E.; Robb, M. A.; Cheeseman, J. R.; Montgomery, J. A.; Vreven, T.; Kudin, K. N.; Burant, J. C.; et al. *Gaussian 03*; Gaussian, Inc.: Wallingford, CT, 2004.

(23) Wang, Y.; Poirier, R. A. Computational Developments in Generalized Valence Bond Calculations. *J. Comput. Chem.* **1996**, *17*, 313−325.

(24) Chattopadhyay, N.; Reva, I.; Lapinski, L.; Fausto, R.; Arnaut, L. G.; Formosinho, S. Photoisomerization of *p*-(Dimethylamino)-*β*-chlorostyrene: A Low Temperature Matrix Isolation FTIR Study. *J. Phys. Chem. A* **2002**, *106*, 3722−3726.

(25) Jeevan, T. S. A.; Nagaraja, K. S. Sublimation Kinetic Studies of the Zr(tmhd)$_4$ Complex. *J. Chem.* **2013**, *2013*, 350937.

(26) Lin, Y.; Wang, H.; Gao, S.; Li, R.; Schaefer, H. F., III. Hydrogen-Bonded Double-Proton Transfer in Five Guanine−Cytosine Base Pairs after Hydrogen Atom Addition. *J. Phys. Chem. B* **2012**, *116*, 8908−8915.

(27) Hargis, J. C.; Vöhringer-Martinez, E.; Woodcock, H. L.; Toro-Labbé, A.; Schaefer, H. F., III. Characterizing the Mechanism of the Double Proton Transfer in the Formamide Dimer. *J. Phys. Chem. A* **2011**, *115*, 2650−2657.

(28) Lopez, J. M.; Männle, F.; Wawer, I.; Buntkowsky, G.; Limbach, H.-H. NMR Studies of Double Proton Transfer in Hydrogen Bonded Cyclic *N,N′*-Diarylformamidine Dimers: Conformational Control, Kinetic HH/HD/DD Isotope Effects and Tunneling. *Phys. Chem. Chem. Phys.* **2007**, *9*, 4498−4513.

(29) Kiselev, V. G.; Cheblakov, P. B.; Gritsan, N. P. Tautomerism and Thermal Decomposition of Tetrazole: High-Level ab Initio Study. *J. Phys. Chem. A* **2011**, *115*, 1743−1753.

(30) Long, G. T.; Brems, B. A.; Wight, C. A. Thermal Activation of the High Explosive NTO: Sublimation, Decomposition, and Autocatalysis. *J. Phys. Chem. B* **2002**, *106*, 4022−4026.

(31) Hammond, G. S. A Correlation of Reaction Rates. "Hammond Postulate". *J. Am. Chem. Soc.* **1955**, *77*, 334−338.

(32) Leffler, J. E. Parameters for the Description of Transition States. *Science* **1953**, *117*, 340−341.

(33) Ismael, A. M.; Cristiano, M. L. S.; Fausto, R.; Gómez-Zavaglia, A. Tautomer Selective Photochemistry in 1-(Tetrazol-5-yl)ethanol. *J. Phys. Chem. A* **2010**, *114*, 13076−13085.

(34) Pagacz-Kostrewa, M.; Reva, I.; Bronisz, R.; Giuliano, B. M.; Fausto, R.; Wierzejewska, M. Conformational Behavior and Tautomer Selective Photochemistry in Low Temperature Matrices: The Case of 5-(1*H*-Tetrazol-1-yl)-1,2,4-triazole. *J. Phys. Chem. A* **2011**, *115*, 5693−5707.